9.4

NUMERICAL SIMULATIONS OF THE 29 JUNE STEPS SUPERCELL

Kristin M. Kuhlman [2,1,*], Edward R. Mansell[2,1], Conrad L. Ziegler[3],
Donald R. MacGorman[3] and Jerry M. Straka[1]
[1]University of Oklahoma, Norman, Oklahoma
[2]Cooperative Institute for Mesoscale Meteorological Studies, Norman, Oklahoma
[3]National Severe Storms Laboratory, Norman, Oklahoma

1. INTRODUCTION

This study focuses on numerical simulations of the 29 June STEPS (Severe Thunderstorm Electrification and Precipitation Study) supercell that produced an F1 tornado and predominately positive ground flashes. The objective is to evaluate the simulated charge structure, lightning flash rate, and polarity against the observed storm and determine the sensitivity of the model to electrification parameterizations. The origins of positive cloud-to-ground (CG) flashes and the relationships between the modeled total flash rate and storm characteristics are of particular interest.

2. MODEL DESCRIPTION

The dynamic cloud model is three dimensional, nonhydrostatic and fully compressible Straka (1989). The model includes prognostic equations for velocity components (momentum), perturbation pressure, potential temperature, turbulent kinetic energy, water vapor and hydrometeor mixing ratios, rime history, and charge variables.

The model employs a microphysics package that includes two liquid hydrometeor categories and ten ice categories distinguished by particle density, habit, and size (Straka and Mansell 2004). The microphysics allows for fractions of mass to move from one category to another depending on droplet collection, riming rate, and melting. Source and sink terms for form and phase changes are included in the microphysics scheme for condensation and evaporation, deposition and sublimation, freezing and melting, aggregation and nucleation, and riming of ice particles, graupel and hail.

The model also includes a choice of parameterizatons for the charging of hydrometeors and a branched lightning parameterization (Mansell et al. 2002). This study uses both inductive and noninductive charging for electrification. The results of laboratory and modeling studies strongly suggest that noninductive charging plays the primary role in producing electrification levels close to that of observed storms (MacGorman and Rust 1998). However, it is believed that inductive charging could also play a role (Brooks and Saunders 1994). Inductive charging occurs in the presence of an electric field, when a rebounding collision occurs between two polarized particles. In the model, inductive charging is only included during graupel-droplet collisions and then only in "dry-growth" mode. Noninductive charging (independent of the electric field) occurs with rebounding collisions between riming graupel and ice particles in the presence of liquid water. The spatial separation of opposite charges on large and small cloud and precipitation particles due to their differential fall speeds generate fields strong enough to produce lightning. For the purpose of this study, the noninductive charging parameterization is based on the laboratory results of Saunders and Peck (1998) (SP98).

3. 29 JUNE AND SIMULATIONS

a. Model Initation

The supercell storm is initiated on an 80 by 80 by 20 km domain. All simulations use a 1 km grid spacing in the horizontal with vertical resolution on a stretched grid ranging from 200 m at the surface to 500 m aloft. The model environment is determined using a modified version of the NCAR mobile GLASS sounding from Goodland, KS (Fig. 1). The sounding is modified in the convective boundary layer (CBL) by increasing the temperature and moisture to better depict the environment where the storm initiated as indicated by surface observations. These mobile mesonet observations in the vicinity of the storm recorded higher temperatures and dewpoints than the mobile sounding earlier that day (E. Rasmussen, personal communication, 2004). The base of the elevated residual layer capping the moist CBL was warmed adiabatically to maintain a minimum concentrated cap strength, thus controlling the spurious growth of instabilities and preserving the mixed layer. The insta-

[*] *Corresponding author address:* Kristin M. Kuhlman, Univ. of Oklahoma, School of Meteorology, Norman, OK 73019; email: kkuhlman@ou.edu

bility of the environment in the modified sounding is thus greatly increased, raising the CAPE from 1370 J kg^{-1} to 2875 J kg^{-1} and lowering the CIN from 100.3 J kg^{-1} to 22.1 J kg^{-1}. The Bulk Richardson Number (BRN), defined as the ratio of the CAPE to the lower tropospheric vertical wind shear, increases from 10.3 to 23.1. The CAPE and BRN of the modified sounding are supportive of possible supercell development (Weisman and Klemp 1982). The model environment is horizontally homogeneous as defined by the modified sounding. A warm bubble ($\Delta\theta = 3\,K$) with randomized thermal perturbations and a radius of 9 km is used to initialize the simulation.

b. Dynamical and Microphysical Evolution

The simulated storm initially develops an elongated multicell structure with successive main updraft cores along the edge of the outflow on the upshear side. By 76 min, the storm has developed a solid core of reflectivity extending to ground with a deep updraft and forward anvil region. During the first 90 min, the storm moves towards the east-northeast. By 90 min, it is hypothesized that storm rotation and the cold pool have intensified sufficiently to force the storm to turn right towards the south and decelerate. The storm continues along a south-southeasterly track for the remainder of the simulation (Fig. 2).

The updraft speed of the simulated storm reaches 30 m s^{-1} at 16 min, it remains strong throughout the simulation and increases to as large as 61 m s^{-1}. The simulated supercell shows evidence of convective surges during its life cycle. The first growth phase occurs at approximately 20 minutes with increases in updraft mass flux and graupel volume (Fig. 3) as well as updraft volume (not shown). Another convective surge occurs at 90 minutes as the storm begins its southerly track. The maximum strength of the storm occurs between 140 and 160 min, when a reflectivity maximum of 69 dBZ is attained. Updraft mass flux and graupel volume also reach a peak during this time. The overall evolution of the simulation is similar to that of the observed storm on 29 June, especially after 90 min. This agreement between the observed and simulated storms is significant as most of the total lightning and virtually all the CG flashes occur after the right turn of the storms.

The timing of the right turn is used as a reference point for comparison between the simulated and observed storms (Fig. 2). The initial development of the observed storm is much slower than the simulations, the latter being intialized by a thermal bubble. The development of the observed and modeled storms is in better agreement from the time of the right turn onward, as supported by visual comparison of results at 90 min of the simulation and 2330 of the observed storm.

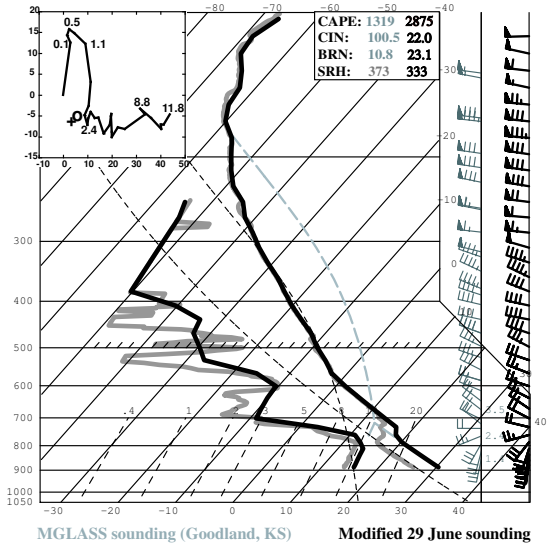

Figure 1: Observed NCAR mobile GLASS sounding released from Goodland, KS at 2022 UTC on 29 June 2000 (thick grey lines). The modified sounding used for model initialization is overlaid (black). The hodograph is the same for both soundings, with corresponding heights (km) AGL denoted. The motion of the observed and modeled storms after developing supercell characteristics is denoted by a plus and a circle respectively. CAPE (J kg^{-1}), CIN (J kg^{-1}), BRN, and 0 to 3 km SRH (m^2 s^{-2}) are shown for both soundings, observed (grey) and modified (black).

c. Electrification

The result of the SP98 scheme at 28 min is a mid-level positive charge with an upper negative charge. As inductive charging and precipitation recycling and fallout quickly develop a lower negative charge region for the third layer, the inverted dipolar charge structure is replaced by an inverted tripolar structure at about 35 min. By 76 min, the storm exhibits an inverted tripole structure with a main mid-level positive charge region with horizontal extent of the charge layers through the storm. A positive surface corona charge layer is also noted at 76 min below 0.5 km AGL. The mature stage of the storm at 116 min depicts a very complex structure with opposite charges occurring at the same altitude (Fig. 5a). The reflectivity core regions continue to maintain a tripolar structure, but outside this region there are five or more vertically stacked charged layers are seen. The overall charge structure is similar to that of an inverted storm as proposed by Marshall et al. (1995) with complexities as described in Stolzenburg et al. (1998).

Simulated intra-cloud (IC) flashes begin at 28 min, with a flash rate of approximately 30 flashes per minute during the first hour (Fig. 4). The IC flash rate reaches a maximum of 264 flashes per min at 120 min and maintains a flash rate above 150 flashes per min during the remainder of the simulation. Lightning leaders travel preferentially through layers of opposite charge, with posi-

tive leaders concentrated in negative charge near 5 km and 13 km. Conversely, mid-levels of the storm are dominated by negative leaders and positive charge.

The SP98 scheme produces a total of 98 positive ground flashes, the first occurring at 67 min, with no negative ground flashes produced. The CG flashes initiate between 5 and 7 km surrounded by the main positive charge region above and a negative charge region below. In the simulation, positive CG flashes are composed of a negative leader traveling upward through positive charge and a positive leader traveling downward through negative charge to ground (Fig. 6). Most simulated lightning flashes exhibit considerable branching by lightning leaders in all directions from the initiation. On occasion, a leader might may go directly to ground, though often a flash goes to ground more than 1 km away (horizontally) from its initiation point. The direction of the path of leaders to ground is dependent on the distribution of charge surrounding the leader. The majority of the CG strikes is located just downshear of the main convective core, though some occur directly under the main updraft.

4. DISCUSSION AND CONCLUSIONS

The bidirectional step-leader model of Mazur and Ruhnke (1993) suggests that lightning is developed between two oppositely charged layers and propagates through opposite polarity charge regions. In the simulations, a positive CG is developed in this way such that negative leaders travel upward through the large positive charge region and positive leaders travel downward through the smaller lower negative charge region to ground. A more in depth look at several ground flashes from the SP98 simulation portrays this development (Fig. 6). Each flash is initiated near where the electric field is maximized between positive and negative charge regions. The positive channel then follows areas of negative charge that have descended towards the ground. The descent of charge to ground appears to be a prerequisite for all simulated ground flashes, allowing the ground flashes to propagate through regions of weak electric potential. The simulation results with SP98 are consistent with the analysis of LMA data from 29 June by Hamlin et al. (2003) (Fig 5). The LMA analysis depicts the initiation and development of positive CGs and the corresponding inferred net charge. This analysis by Hamlin et al. (2003) points to the importance of the polarity of the lowest charge region for the polarity of the ground flashes.

Lightning flashes have qualitatively similar morphological characteristics in both the observed and simulated storms. Both the LMA observations and the model simulations depict normal polarity cloud flashes initiating between an upper positive and lower negative charge regions and inverted polarity flashes initiating below negative charge and above positive charge. The observations and the simulations also reveal that the lowest charge region must be negative to produce positive ground flashes in the convective core, a result that was noted by Mansell et al. (2002) in previous thunderstorm simulations. Though ground flashes seem to be correlated to areas of descending charge at very low levels (probably associated with precipitation cores), it is presently unclear if this correlation could be used to predict the exact timing and location of ground flashes due to their inherent stochastic nature.

Fluctuations of convective and precipitation intensity correlate positively with changes of the total flash rate. The correlation between intensity and flash rate is forced by the noninductive charging and the subsequent three-dimensional recycling motions of the charged hydrometeors. The model results agree with observations that the total flash rate–rather than ground flash rate or polarity–provides the most robust electrical representation of the microphysical and kinematic intensity of storms that are sufficiently deep for development of updrafts in the mixed phase region.

4. ACKNOWLEDGEMENTS

Support for this research was provided by the National Science Foundation grant ATM-0119398.

References

Brooks, I. M. and C. P. R. Saunders, 1994: An experimental investigation of the inductive mechanism of thunderstorm electrification. *J. Geophys. Res.*, **99**, 10627–10632.

Hamlin, T., P. R. Krehbiel, R. J. Thomas, W. Rison, and J. Harlin, 2003: Electrical structure and storm severity inferred by 3-D lightning mapping observations during STEPS. *Proceedings, 12th Int. Conf. on Atmospheric Electricity*, ICAE, Versailles, France, 189–192.

MacGorman, D. R. and W. D. Rust, 1998: *The electrical nature of storms*. Oxford University Press, 422 pp.

Mansell, E. R., D. MacGorman, C. L. Ziegler, and J. M. Straka, 2002: Simulated three-dimensional branched lightning in a numerical thunderstorm model. *J. Geophys. Res.*, **107**, doi:10.1029/2000JD000244.

Marshall, T. C., M. P. McCarthy, and W. D. Rust, 1995: Electric field magnitudes and lightning initiation in thunderstorms. *J. Geophys. Res.*, **100**, 7097–7103.

Mazur, V. and L. Ruhnke, 1993: Common physical processes in natural and artificially triggered lightning. *J. Geophys. Res.*, **98**, 913–930.

Saunders, C. P. R. and S. L. Peck, 1998: Laboratory studies of the influence of the rime accretion rate on charge transfer during crystal/graupel collisions. *J. Geophys. Res.*, **103**, 13949–13956.

Stolzenburg, M., W. D. Rust, and T. C. Marshall, 1998: Electrical structure in thunderstorm convective regions 3. Synthesis. *J. Geophys. Res.*, **103**, 14097–14108.

Straka, J. M., 1989: *Hail Growth in a Highly Glaciated Central High Plains Multi-cellular Hailstorm*. Ph.D. thesis, University of Wisconsin-Madison, Dept. of Meteorology, Madison, WI, 53706.

Straka, J. M. and E. R. Mansell, 2004: A bulk microphysics parameterization with multiple ice precipitation categories. *In review at J. Appl. Meteor.*.

Weisman, M. L. and J. B. Klemp, 1982: The dependence of numerically simulated convective storms on vertical wind shear and buoyancy. *Mon. Wea. Rev.*, **110**, 504–520.

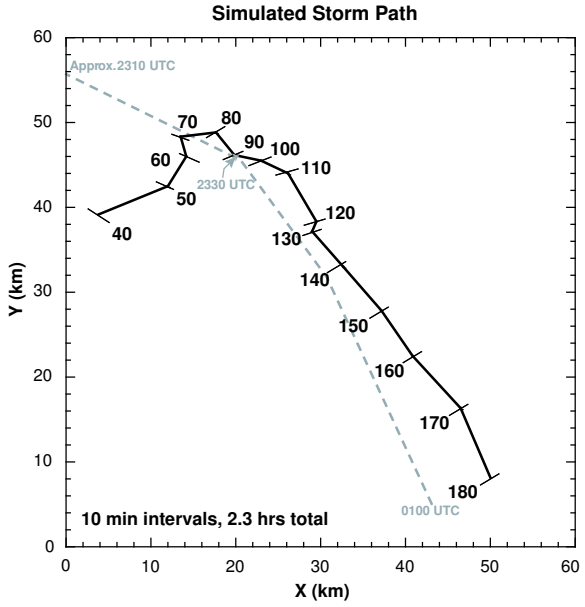

Figure 2: Simulated storm path for 2.3 h. Position of storm shown every 10 min starting at 40 min after initiation. Observed storm path (grey dash line) relative to model path from 2300 UTC through 0100 UTC.

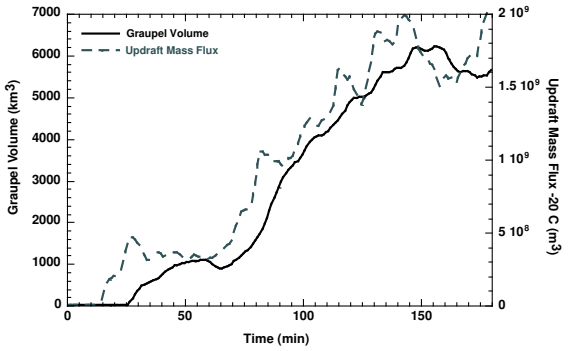

Figure 3: Time series of graupel volume (km^3) (black) and updraft mass flux through $-20°C$ (m^3) (grey).

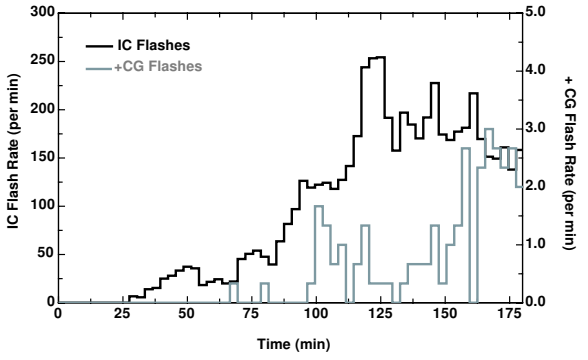

Figure 4: Lightning flash rate for the SP98 simulation. In-cloud flashes per min (black) and positive cloud-to-ground flashes per min (grey).

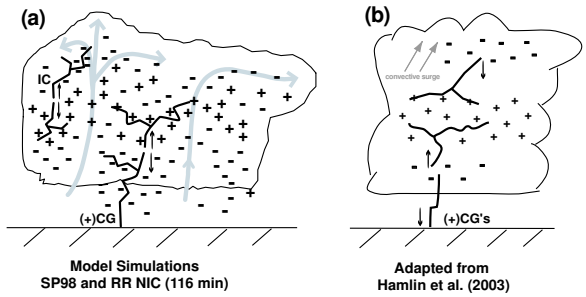

Figure 5: Charge structure from: (a) SP98 simulation at 116 min, airflow shown by grey streamlines; typical IC and +CG in black (b) observations of 29 June once the storm had developed supercell characteristics, from Hamlin et al. (2003) with leaders and charge structure inferred from LMA activity.

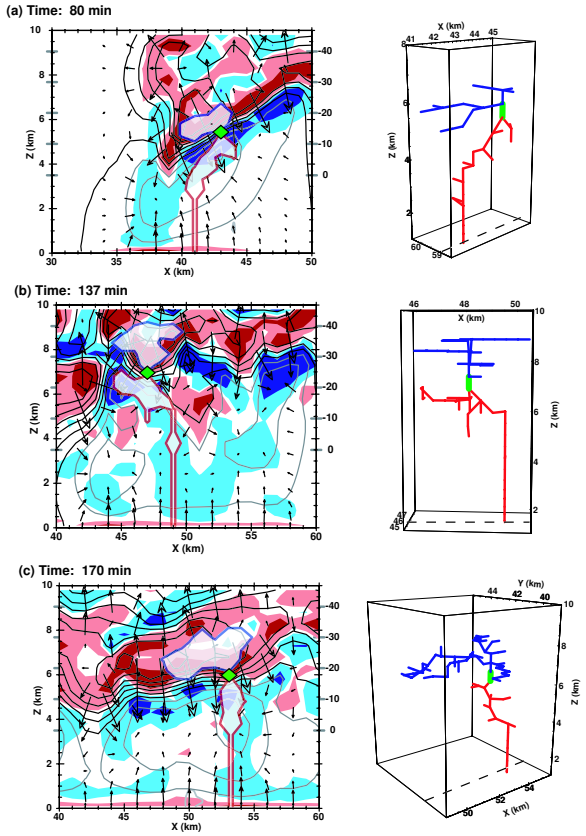

Figure 6: Three positive CG flashes from SP98 model simulation at: (a) 80 min; (b) 137 min; (c) 170 min. Left panels: Vertical cross-section through storm. Positive and negative charge regions are contoured in solid red and blue respectively, vectors are of the electric field, black and grey contours indicate equipotential lines. Lightning leaders in white fill contour, positive with red outline, negative with blue outline. Right panels: 3-D view of each flash, initiations shown in green, positive leaders in red and negative leaders in blue. Location of x-z cross-section shown in left panel denoted by grey-dashed line.